

Search for optimum labeling schemes in qubit systems for quantum-information processing by nuclear magnetic resonance

Ranabir Das,¹ Sukhendu Chakraborty,^{2,*} K. Rukmani,^{1,†} and Anil Kumar^{1,2,‡}

¹*Department of Physics, Indian Institute of Science, Bangalore, India*

²*Sophisticated Instruments Facility, Indian Institute of Science, Bangalore, India*

(Received 4 February 2004; published 29 July 2004)

Optimal labeling schemes lead to efficient experimental protocols for quantum-information processing by nuclear magnetic resonance (NMR). A systematic approach to finding optimal labeling schemes for a given computation is described here. The scheme is described for both quadrupolar systems and spin- $\frac{1}{2}$ systems. Using the technique of transition selective pulses, one of the optimal labeling schemes has been applied to experimentally implement a quantum full adder in a four-qubit system by NMR.

DOI: 10.1103/PhysRevA.70.012314

PACS number(s): 03.67.Lx

I. INTRODUCTION

Quantum computers can solve certain problems that are intractable with the classical computers [1,2]. Several quantum algorithms have been devised which use the quantum-mechanical properties of the physical systems to solve problems with more speed and fewer resources [3–5]. Implementation of the quantum algorithm requires a coherent control over the physical systems that are used for computation. Therefore, a great deal of emphasis is laid on simplification of experimental schemes, so as to retain coherent control and avoid errors [6–8]. Among the various techniques, nuclear magnetic resonance (NMR) has emerged as a suitable technique for the demonstration of quantum information processing with a small number of qubits [9–19]. In liquid-state NMR, information processing is carried out by the use of spin- or qubit-selective pulses separated by evolutions under the system Hamiltonian [2,10], or by the use of transition-selective pulses along with qubit-selective pulses [14,20–23]. Transition-selective pulses are radiofrequency pulses tuned to the resonance frequency of a selected single-quantum transition, causing irradiation at a specific line of the spectrum without perturbing others. A transition-selective π pulse tuned at a specific transition exchanges the amplitudes between the two eigenstates. Such pulses can be used to simplify the implementation of several logical operations. For example, in an N -qubit system, a controlled $N-1$ -NOT gate requires a complex pulse sequence with a series of qubit-selective pulses separated by Hamiltonian evolutions [11], whereas it requires only one transition-selective π pulse between the states $|111\cdots 10\rangle$ and $|111\cdots 11\rangle$ [24].

Recently, it has been shown that relabeling of states simplifies the experimental protocol of certain operations [21,22]. While implementing half-adder and subtractor operations in a quadrupolar system, relabeling led to an effi-

cient experimental scheme that requires fewer pulses than the conventional labeling [21]. The idea behind relabeling is as follows: For spin- $\frac{1}{2}$ systems, conventional labeling (CL) uses the following logic. The state in which all the spins are in an identical state, such as $|\alpha\alpha\alpha\cdots\alpha\rangle$, is labeled as $|000\cdots 0\rangle$ and each spin flip is labeled as a bit flip, namely $|\alpha\beta\alpha\cdots\alpha\rangle = |010\cdots 0\rangle$. This scheme labels each state with a well-identified label and leads to the identification of a spin as a qubit. Spin-selective pulses then act as qubit-selective pulses and many pulse schemes have been developed which use spin- (or qubit-) selective pulses along with Hamiltonian (or exchange coupling, J) evolution periods [2,9,10]. On the other hand, quantum information processing (QIP) has also been demonstrated using nuclei with spins $> \frac{1}{2}$, retaining their quadrupolar couplings by partially orienting molecules in liquid crystalline media [25]. In such systems, a spin is no longer a qubit. However, it has been demonstrated that the 2^N nondegenerate energy levels of such a system can be utilized as an N -qubit system. So far, only spins $\frac{3}{2}$ and $\frac{7}{2}$ have been used, respectively, yielding two and three qubits [20–22,25–28]. Furthermore, in such systems, a bit flip is not a spin flip while it can be treated as a qubit flip. One can follow a CL scheme in which the lowest (or highest) energy level can be given the label $|000\cdots 0\rangle$ and each subsequent level can be labeled in increasing order of binary numbers (CL) or single bit flips (Gray code), as shown in Table I. It was conjectured earlier that all such schemes are acceptable as long as a single label is attached to each level and the scheme is retained throughout a given set of computations [21,22]. Indeed, it was demonstrated that it is acceptable to search for “optimum labeling schemes” (OLS) such that a minimum number of unitary transforms is needed for a given set of computations [21].

The utility of OLS is explained in the following: A transition-selective pulse has low power and small bandwidth and it excites a selected single-quantum transition. That is, it can cause an operation between two states which differ by $\Delta m = \pm 1$, where m is the magnetic quantum number. Suppose an operation requires a transformation between two states (A and B) which differ by $\Delta m \neq \pm 1$. Then a single transition-selective π pulse will not suffice. One then looks for some intermediate eigenstate or eigenstates which differ by $\Delta m = \pm 1$ and connect A and B . A sequence of transition-

*Present address: Department on Computer Science, Duke University, Durham, NC, USA.

†Present address: Department of Physics, Bangalore University, Bangalore, India.

‡Corresponding author: Email address: anilnmr@physics.iisc.ernet.in

TABLE I. Conventional labeling (CL), gray code, and optimum labeling (for half-adder and subtracter operation) in a spin-7/2 system.

Energy level	A	B	C
m	CL	Gray	Optimum
$\frac{7}{2}$	000	000	000
$\frac{5}{2}$	001	001	010
$\frac{3}{2}$	010	011	011
$\frac{1}{2}$	011	010	001
$-\frac{1}{2}$	100	110	101
$-\frac{3}{2}$	101	100	110
$-\frac{5}{2}$	110	101	111
$-\frac{7}{2}$	111	111	100

selective π pulses transforms these two states via the intermediate states. However, one can always relabel the energy levels such that A and B are two levels connected by $\Delta m = \pm 1$. A single transition-selective π pulse would then suffice. With this logic, one can find an optimal labeling scheme which reduces the computation to a minimum number of such transition-selective pulses.

The optimum labeling scheme for the half-adder and subtracter using an oriented spin- $\frac{7}{2}$ (three-qubit) system given in column C of Table I was found by trial and error [21]. However, by no means is this scheme unique; there must be many more labeling schemes with equal efficiency. Furthermore, for higher-qubit systems the trial and error method will become laborious and inefficient. Therefore, there is a need for a systematic approach to this problem of finding an optimum labeling scheme for a given computation or a set of computations. This paper deals with one such approach. Section II outlines a protocol to search for optimum labeling schemes, Sec. III introduces full-adder operation, Sec. IV gives the protocol to search for optimum labeling schemes in the case of multiple operations with an example of a full adder +swap2, 4, and Sec. V contains an experimental implementation of a full adder by a four-qubit weakly coupled spin- $\frac{1}{2}$ system.

The relabeling scheme described here is applicable to arithmetic operations and logic gates, which have a one-to-one mapping between initial and final states. This does not

TABLE II. Truth table for a certain logical operation.

Input				Output			
X_1	X_2	X_3	X_4	Y_1	Y_2	Y_3	Y_4
0	0	0	0	0	0	0	0
0	0	0	1	0	0	0	1
0	0	1	0	0	0	1	0
0	0	1	1	0	0	1	1
0	1	0	0	0	1	1	0
0	1	0	1	0	1	1	1
0	1	1	0	0	1	0	1
0	1	1	1	0	1	0	0
1	0	0	0	1	0	1	0
1	0	0	1	1	0	1	1
1	0	1	0	1	0	0	1
1	0	1	1	1	0	0	0
1	1	0	0	1	10	1	
1	1	0	1	1	1	0	0
1	1	1	0	1	1	1	1
1	1	1	1	1	1	1	0

include operations which create superposition, such as the Hadamard gate. Relabeling schemes for such operations and quantum algorithms may require a different strategy.

II. OPTIMUM LABELING SCHEME

To search for optimum labeling schemes (OLS) in logic gates and arithmetic operations, we start with the truth table of a computation. Table II contains a particular truth table for a four-qubit system. At this moment it is not important to know the logical operation this truth table represents. The table is needed to illustrate the procedure. We search for OLS with the help of set theory. We consider that all the states of the system constitute a universal set $\{S\}$. Then from the truth table, we construct maximal sets $\{S_i\}$ which are mutually exclusive subsets of $\{S\}$. To construct maximal sets, the first input state is taken up and put in the first set $\{S_1\}$. The corresponding output is noted and is added to $\{S_1\}$ if it is not already included in it (Table III). This process is continued until we reach a state whose output is the first element of $\{S_1\}$. Then the set $\{S_1\}$ is completed. In the present case, the $\{S_1\}$ set contains only one element $|0000\rangle$ since it transform

TABLE III. Construction of maximal sets for the operation of Table II.

Chains	Maximal sets
$ 0000\rangle$	$S_1=\{ 0000\rangle\}$
$ 0001\rangle$	$S_2=\{ 0001\rangle\}$
$ 0010\rangle$	$S_3=\{ 0010\rangle\}$
$ 0011\rangle$	$S_4=\{ 0011\rangle\}$
$ 0100\rangle \rightarrow 0110\rangle \rightarrow 0101\rangle \rightarrow 0111\rangle \rightarrow 0100\rangle$	$S_5=\{ 0100\rangle, 0110\rangle, 0101\rangle, 0111\rangle\}$
$ 1000\rangle \rightarrow 1010\rangle \rightarrow 1001\rangle \rightarrow 1011\rangle \rightarrow 1000\rangle$	$S_6=\{ 1000\rangle, 1010\rangle, 1001\rangle, 1011\rangle\}$
$ 1100\rangle \rightarrow 1101\rangle \rightarrow 1100\rangle$	$S_7=\{ 1100\rangle, 1101\rangle\}$
$ 1110\rangle \rightarrow 1111\rangle \rightarrow 1110\rangle$	$S_8=\{ 1110\rangle, 1111\rangle\}$

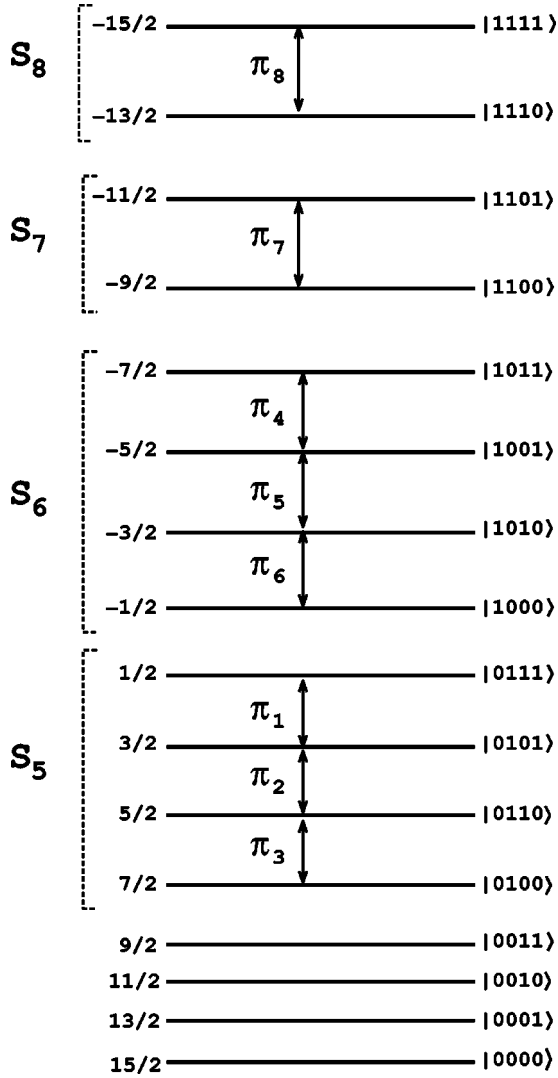


FIG. 1. The Zeeman energy levels of a spin- $\frac{15}{2}$ nucleus along with one of the optimum labeling schemes for the logical operation given in Table II. The magnetic quantum number (m) corresponding to each eigenstate is given on the left-hand side, and the qubit labeling is given on the right-hand side. The maximal sets of Table III are shown in the energy-level diagram along with the transition selective π pulses required to implement the truth table of Table II using this labeling scheme.

into itself. Similarly, sets $\{S_2\}$, $\{S_3\}$, and $\{S_4\}$ each contain one element. The set $\{S_5\}$ is formed by noting that $|0100\rangle \rightarrow |0110\rangle \rightarrow |0101\rangle \rightarrow |0111\rangle \rightarrow |0100\rangle$. This process is carried out for all $\{S_j\}$ by selecting an input state not forming a part of previous $\{S_j\}$'s, and it is continued until all the states are included in exactly one of the maximal sets $\{S_j\}$ (Table III). It is evident that the maximal sets $\{S_j\}$ are mutually exclusive.

An optimum labeling scheme for executing the logical operation of Table II by single-quantum transition-selective pulses is obtained by arranging the labels of levels in the same order as in column 1 of Table III. The number of pulses for any set $\{S_j\}$ will be $|S_j|-1$, where $|S_j|$ is the cardinality (number of elements) of the set. Thus the minimum number of pulses required for the execution of the logical operation of Table II is

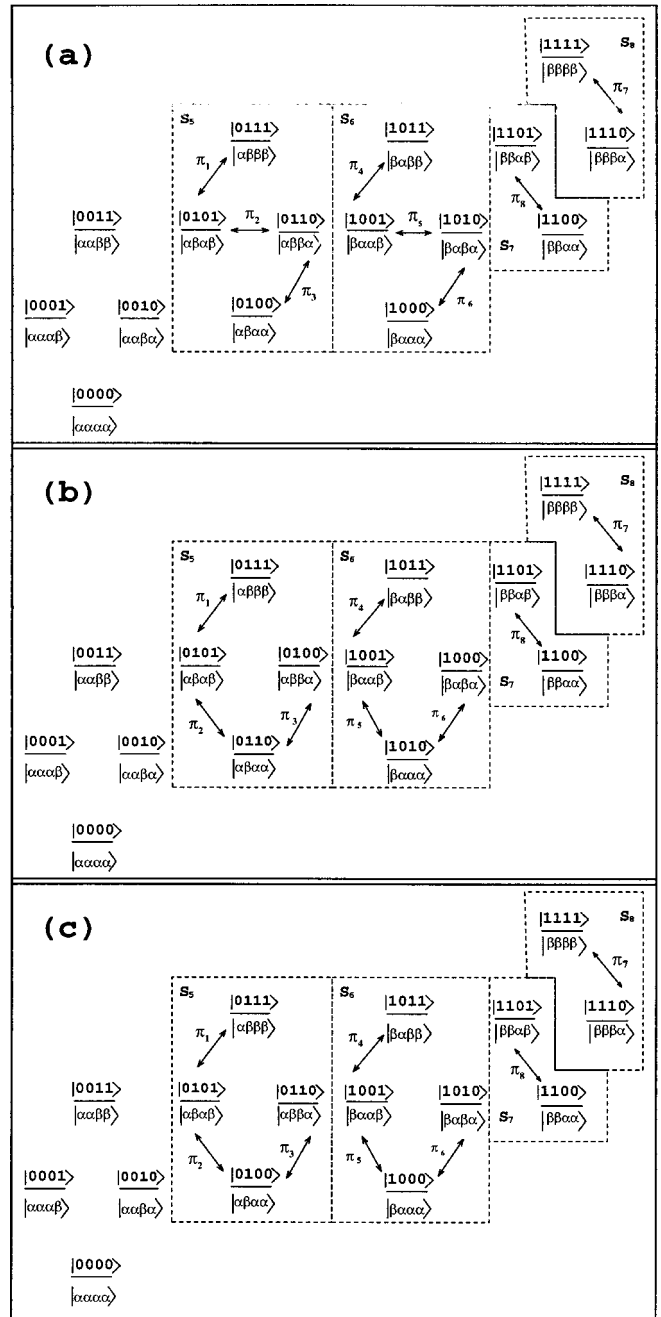


FIG. 2. (a) Conventional labeling scheme and the pulses required for implementing the truth table of Table II in a four-qubit spin- $\frac{1}{2}$ system. (b) Relabeled energy levels to implement the truth table of Table II with optimum pulses. (c) The conventional scheme of (a) by rearranging the sequence of pulses to implement the logic of Table II with the minimum number of pulses.

$$N_p = \sum_{i=1}^M (|S_i| - 1), \quad (1)$$

where M is the number of maximal sets. In the present example, the number of transition-selective pulses needed is $3+3+1+1=8$. It may be pointed out that implementation of this operation in a quadrupolar system using conventional

TABLE IV. Truth table of a classical full adder.

C_0	A	B	S	C_1
0	0	0	0	0
0	0	1	1	0
0	1	0	1	0
0	1	1	0	1
1	0	0	1	0
1	0	1	0	1
1	1	0	0	1
1	1	1	1	1

labeling or the gray code would require 12 or 10 transition-selective pulses, respectively.

After creating the maximal sets, one has to consider only those sets that have more than one element, as they are the ones that would require “pulses.” We have seen that in a maximal set, transformations between the states take place in a chain. This chain of states should be mapped to a chain of energy levels where each level in the chain should be connected to its previous and next level by single-quantum transitions. Mapping the sets to the subspace of energy levels should start with the mapping of a set having the largest number of elements (i.e., max. cardinality) and then move in a decreasing order. This mapping follows different strategies for quadrupolar systems and coupled spin- $\frac{1}{2}$ systems. These are outlined in the following.

A. Optimum labeling for quadrupolar systems

The Hamiltonian of a quadrupolar nucleus partially oriented in a liquid-crystalline matrix, in the presence of a large magnetic field B_0 and having a first-order quadrupolar coupling, is given by [33]

$$\begin{aligned} \mathcal{H} &= \mathcal{H}_Z + \mathcal{H}_Q = -\omega_0 I_z + \frac{e^2 q Q}{4I(2I-1)} (3I_z^2 - I^2) S \\ &= -\omega_0 I_z + \Lambda (3I_z^2 - I^2), \end{aligned} \quad (2)$$

where $\omega_0 = \gamma B_0$ is the resonance frequency, γ being the gyromagnetic ratio, S is the order parameter at the site of the nucleus, $e^2 q Q$ is the quadrupolar coupling, and $\Lambda = e^2 q Q S / [4I(2I-1)]$ is the effective quadrupolar coupling. Though $e^2 q Q$ is of the order of several MHz, a small value for the order parameter (S) converts the effective quadrupolar coupling “ Λ ” into several kHz. In such circumstances, a spin- I nucleus has $2I+1$ nonequispaced eigenstates and $2I$ well-resolved single-quantum transitions separated by effective quadrupolar coupling “ Λ .” Recently, it has been demonstrated that such a system can be treated as an N -qubit system, provided $(2I+1) = 2^N$ [25]. For example a single spin- $\frac{3}{2}$ acts as a two-qubit system and a spin- $\frac{7}{2}$ acts as a three-qubit system [20,21,25–28].

In quadrupolar systems, the energy levels are in increasing order of Zeeman energy. Each level is connected to adjacent levels by single-quantum transitions, yielding $2^N - 1$ single-quantum transitions. This puts certain constraints in

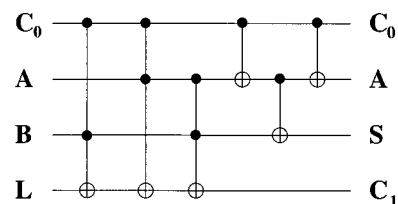


FIG. 3. Circuit of a quantum full adder. The two bits A and B are added with a carry “ C_0 ” from the previous operation. An ancillary bit L is included in the input to make the operation reversible. After the full-adder operation, the sum gets stored in S ($S = C_0 \oplus A \oplus B$), and the carry is stored in C_1 [$C_1 = L \oplus (AB \oplus AC_0 \oplus BC_0)$].

identification of maximal sets with the energy levels. An example of a labeling scheme for the operation in Table II is given in Fig. 1. The maximal sets are shown in the energy-level diagram along with the transition-selective π pulses which are required to implement the truth table of Table II in this labeling scheme. Let us take the case of S_5 , which has four states. They are being mapped in a subspace of the energy-level diagram to four energy levels that are in a chain. Then the required transformations can be achieved by three π pulses applied in the reverse order of the chain. Hence the pulses are to be applied in the order $(\pi_1 \pi_2 \pi_3)$, as shown in Fig. 1,

$$\begin{aligned} & (\pi_1)_y^{|0111\rangle \leftrightarrow |0101\rangle} (\pi_2)_y^{|0101\rangle \leftrightarrow |0110\rangle} (\pi_3)_y^{|0110\rangle \leftrightarrow |0100\rangle} \\ &= \begin{pmatrix} 1 & 0 & 0 & 0 \\ 0 & 0 & 0 & 1 \\ 0 & 0 & 1 & 0 \\ 0 & -1 & 0 & 0 \end{pmatrix} \begin{pmatrix} 1 & 0 & 0 & 0 \\ 0 & 0 & 1 & 0 \\ 0 & -1 & 0 & 0 \\ 0 & 0 & 0 & 1 \end{pmatrix} \begin{pmatrix} 0 & 0 & 1 & 0 \\ 0 & 1 & 0 & 0 \\ -1 & 0 & 0 & 0 \\ 0 & 0 & 0 & 1 \end{pmatrix} \\ &= \begin{pmatrix} 0 & 0 & 1 & 0 \\ 0 & 0 & 0 & 1 \\ 0 & -1 & 0 & 0 \\ 1 & 0 & 0 & 0 \end{pmatrix}. \end{aligned} \quad (3)$$

The above operator is for a subsystem of the last two qubits in the four-qubit system, where the first two qubits are in the $|01\rangle$ state. S_6 also has a similar chain which is then mapped to a chain of levels as shown in Fig. 1. S_7 has a chain of two states and it can be mapped onto any two adjacent energy levels of the system. S_8 follows the same logic. The energy levels corresponding to states of S_7 and S_8 in our labeling scheme are given in Fig. 1. However, the relabeling scheme of Fig. 1 is not unique; many optimum labeling schemes are possible.

The basic idea of relabeling is that the 2^N energy levels of an N -qubit system can be given desired labels. If the only necessary condition is that one label is attached to each energy level, then there are $2^N!$ possibilities. However, only a few of these are optimal. In the case of a quadrupolar system, all the energy levels differ in their energy by at least one Larmor frequency. Thus, the number of different OLS possible in quadrupolar system is a permutation of the different maximal sets, multiplied by the allowed permutations of elements in each set. However, for sets with more than one

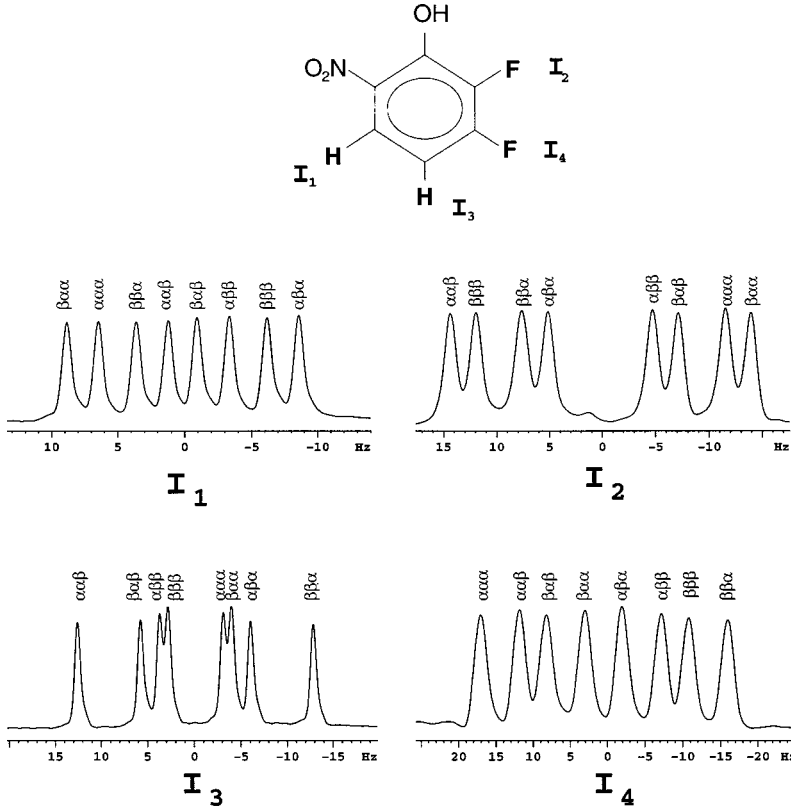


FIG. 4. The four-qubit system of 2–3 difluoro 6-nitrophenol. The two protons (I_1 and I_3) and the two fluorine nuclei (I_2 and I_4) constitute the four-qubit system. The equilibrium spectrum of each nucleus is individually shown. The assignment of the transitions is given above each line, which has been determined by transition tickling and HET-Z-COSY experiments [29,30]. Each assignment identifies a transition of the spin corresponding to the states of other spins. In a 500 MHz spectrometer, the chemical shift difference between the two fluorine spins is 16 kHz while that between the two protons is 250 Hz. The couplings range from 19.1 Hz to -2.3 Hz.

element, optimal labeling demands that the order of states must be the same as that of the transformations. Thus, only two permutations of states are allowed in each set, either in ascending or descending order of energy. Hence the total number of optimal labeling schemes is

$$P = M! 2^k, \quad (4)$$

where k is the number of maximal sets with more than one cardinal number. We note that for the example of Table I, the number of OLS is $8! \times 2^4 = 645\,120$ out of a total of $16! \cong 2 \times 10^{13}$ possible labeling schemes.

B. Optimum labeling for spin- $\frac{1}{2}$ systems

When placed in a magnetic field (B_o), the energy levels of a spin- $\frac{1}{2}$ nucleus are split into two. These energy levels can be labeled as $|0\rangle$ and $|1\rangle$ and hence a spin- $\frac{1}{2}$ nucleus acts as a qubit. N such nuclei, having different Larmor frequencies and coupled to each other by indirect spin-spin interaction, constitute an N -qubit system. The Hamiltonian for such a system is given by [11]

$$\mathcal{H} = \mathcal{H}_Z + \mathcal{H}_J = \sum_i \omega_i I_{iz} + \sum_{i,j(i<j)} 2\pi J_{ij} \vec{I}_i \cdot \vec{I}_j, \quad (5)$$

where \mathcal{H}_Z is the Zeeman Hamiltonian, \mathcal{H}_J is the coupling Hamiltonian, $\omega_i = \gamma_i B_o$ is the Larmor frequency of the i th spin, and J_{ij} is the coupling between the i th and j th spin. When $2\pi J_{ij} \ll |\omega_i - \omega_j|$, the system is said to be weakly coupled, and the Hamiltonian can be approximated to [11]

$$\mathcal{H} = \sum_i \omega_i I_{iz} + \sum_{i,j(i<j)} 2\pi J_{ij} I_{iz} I_{jz}. \quad (6)$$

Under the approximation of Eq. (6), products of eigenstates of individual spins are the eigenstates of the system, and a spin can be treated as a qubit [9,10]. In this paper, we restrict to such systems. In such cases, for an N -qubit spin- $\frac{1}{2}$ system there are N single-quantum transitions from each energy level, amounting to a total of $N2^{N-1}$ single-quantum transitions. Hence the number of possible optimal labeling schemes is much larger than the quadrupolar system described above. It turns out that in such cases, the conventional labeling scheme may be an optimum scheme with some minor modifications. For example, Fig. 2(a) contains a conventional labeling scheme and the pulses needed for implementing the operation of Table II. Note that in the maximal set S_5 , the transformations require three pulses— π_1 , π_2 , followed by π_3 —whose operator is

$$\begin{aligned} & (\pi_1)_y^{|0101\rangle \leftrightarrow |0111\rangle} (\pi_2)_y^{|0101\rangle \leftrightarrow |0110\rangle} (\pi_3)_y^{|0110\rangle \leftrightarrow |0100\rangle} \\ &= \begin{pmatrix} 1 & 0 & 0 & 0 \\ 0 & 0 & 0 & 1 \\ 0 & 0 & 1 & 0 \\ 0 & -1 & 0 & 0 \end{pmatrix} \begin{pmatrix} 1 & 0 & 0 & 0 \\ 0 & 0 & 1 & 0 \\ 0 & -1 & 0 & 0 \\ 0 & 0 & 0 & 1 \end{pmatrix} \begin{pmatrix} 0 & 0 & 1 & 0 \\ 0 & 1 & 0 & 0 \\ -1 & 0 & 0 & 0 \\ 0 & 0 & 0 & 1 \end{pmatrix} \\ &= \begin{pmatrix} 0 & 0 & 1 & 0 \\ 0 & 0 & 0 & 1 \\ 0 & -1 & 0 & 0 \\ 1 & 0 & 0 & 0 \end{pmatrix}. \end{aligned} \quad (7)$$

The above operator is for a subsystem of the last two qubits in the four-qubit system, where the first two qubits are in the $|01\rangle$ state. However, the transformation of π_2 is between two states $|0101\rangle$ and $|0110\rangle$ which differ by $\Delta m=0$, and cannot be accomplished by one single-quantum transition-selective pulse. Hence it would seem that the experimental protocol would require more pulses. Relabeling can reduce the number of pulses. Figure 2(b) shows a relabeled scheme where the labels of the states ($\alpha\beta\beta\alpha$ and $\alpha\beta\alpha\alpha$) as well as ($\beta\alpha\alpha\alpha$ and $\beta\alpha\beta\alpha$) are interchanged so that $|0101\rangle \leftrightarrow |0110\rangle$ and $|1001\rangle \leftrightarrow |1010\rangle$ are connected by single-quantum transitions.

However, in this case we observe that, by changing the sequence of pulses, one can achieve the same transformations of S_5 and S_6 in a conventional labeling scheme with a minimum number of pulses. For example, in the maximal set S_5 , we can change the sequence of pulses as π_1 , π_3 , followed by π_2 , where π_2 is applied between the states $|0100\rangle$ and $|0101\rangle$ [as shown in Fig. 2(c)]. Then the operator is the same as that of Eq. (7),

$$\begin{aligned} & (\pi_1)_y^{|0101\rangle \leftrightarrow |0111\rangle} (\pi_3)_y^{|0110\rangle \leftrightarrow |0100\rangle} (\pi_2)_y^{|0100\rangle \leftrightarrow |0101\rangle} \\ &= \begin{pmatrix} 1 & 0 & 0 & 0 \\ 0 & 0 & 0 & 1 \\ 0 & 0 & 1 & 0 \\ 0 & -1 & 0 & 0 \end{pmatrix} \begin{pmatrix} 0 & 0 & 1 & 0 \\ 0 & 1 & 0 & 0 \\ -1 & 0 & 0 & 0 \\ 0 & 0 & 0 & 1 \end{pmatrix} \begin{pmatrix} 0 & 1 & 0 & 0 \\ -1 & 0 & 0 & 0 \\ 0 & 0 & 1 & 0 \\ 0 & 0 & 0 & 1 \end{pmatrix} \\ &= \begin{pmatrix} 0 & 0 & 1 & 0 \\ 0 & 0 & 0 & 1 \\ 0 & -1 & 0 & 0 \\ 1 & 0 & 0 & 0 \end{pmatrix}. \end{aligned} \quad (8)$$

This sequence will require only three single-quantum pulses since all the pulses are between eigenstates with $\Delta m = \pm 1$. Similarly in set S_6 , π_4 , π_6 , followed by π_5 will suffice [Fig. 2(c)]. In this protocol, the conventional labeling scheme requires a total of eight pulses for implementing the truth table of Table II, which is identical to OLS. Thus, the conventional scheme is also optimum. It turns out that for experimental convenience, relabeling may still be useful, as will be shown in Sec. V.

It may be noted from Eqs. (3), (7), and (8), that the collective operator of the three transition-selective pulses differs from the ideal operator of the transformations in S_5 by a controlled phase factor [10]. If one starts from an equilibrium state, the results are identical to that of the operation of Table II. When applied to a pure state, the phase factor must either be taken into consideration or be corrected by adding a controlled phase gate, using transition-selective z pulses [23].

III. FULL ADDER

Table II is the truth table of a quantum full adder. The full adder is a basic component of conventional computers. The quantum full adder is also an important part of many quantum algorithms. In particular, it is a key step in Shor's prime factorization algorithm, where it is necessary to perform modular exponentiation $f(x) = a^x \bmod M$ [3]. A classical full adder (Table IV) adds bits "A" and "B" and carry "C₀" to

give a sum "S" and a carry "C." This operation is not reversible. Quantum full adder, however, needs to be reversible. An extra ancillary bit is added in the input "L" to make the operation reversible. The truth table then becomes exactly the one given in Table II, where $X_1 = C_0$, $X_2 = A$, $X_3 = B$ and $X_4 = L$, $Y_1 = C_0$, $Y_2 = A$, Y_3 is the sum ($= C_0 \oplus A \oplus B = S$), and Y_4 is the carry [$= L \oplus (AB \oplus AC_0 \oplus BC_0) = C_1$]. Figure 3 contains the circuit for the quantum full adder and Fig. 1 has one of the many possible optimum labeling schemes for the quantum full adder in a four-qubit (spin- $\frac{15}{2}$) quadrupolar system.

IV. MULTIPLE OPERATIONS

The optimal labeling for a sequence of logical operations can be constructed in a manner similar to the one outlined in Sec. II. For example, if one wishes to implement a swap operation between the second and fourth qubit after implementing full adder, then the maximal sets have to be constructed from the truth table of combined operation of full adder+swap 2,4. For full adder+swap-2,4, the maximal sets are $S_1 = \{|0000\rangle\}$, $S_2 = \{|0001\rangle, |0100\rangle, |0011\rangle, |0110\rangle, |0101\rangle, |0111\rangle\}$, $S_3 = \{|0010\rangle\}$, and $S_4 = \{|1000\rangle, |1010\rangle, |1100\rangle, |1101\rangle, |1001\rangle, |1110\rangle, |1111\rangle, |1011\rangle\}$. For implementing full adder+swap 2,4 in a four-qubit quadrupolar system, this labeling scheme would require 12 transition-selective pulses. Often various logical operations do not commute. For example, full adder and swap 2,4 do not commute. Hence, if one wants to implement the operations in the reverse order, namely swap 2,4+full adder, the truth table of the combined operation is different and so is the order of elements in the maximal sets: $S_1 = \{|0000\rangle\}$, $S_2 = \{|0001\rangle, |0110\rangle, |0011\rangle, |0101\rangle, |0111\rangle, |0100\rangle\}$, $S_3 = \{|0010\rangle\}$, and $S_4 = \{|1000\rangle, |1010\rangle, |1001\rangle, |1101\rangle, |1100\rangle, |1011\rangle, |1111\rangle, |1110\rangle\}$. However, it is evident that swap 2,4+full adder also requires 12 transition-selective pulses. It may be mentioned that the implementation of full adder+swap 2,4 by CLS would require 24, and the gray code would require 26 transition-selective pulses in a four-qubit quadrupolar system.

V. EXPERIMENT

The molecule 2-3 difluoro 6-nitrophenol (dissolved in $\text{CDCl}_3 + 1$ drop D_2O) has four weakly coupled spin- $\frac{1}{2}$ nuclei, acts as a four-qubit system, and was chosen to implement the quantum full adder (Fig. 4). The proton of the phenol group is exchanged with the D_2O . The two remaining protons and the two fluorine nuclei constitute the four-qubit system. The equilibrium spectrum of each nucleus is given in Fig. 4. In a 500 MHz NMR spectrometer, the chemical shift difference between the two fluorine spins is 16 kHz while that between the two protons is 250 Hz. The couplings range from 19.1 Hz to -2.3 Hz. The assignment of transitions given in Fig. 4 using the energy-level diagram (Fig. 5) was obtained with two independent methods. In method (i) a transition-selective tickling experiment was performed individually for all the 32 transitions to yield the assignment of transitions [29]. In method (ii) a two-dimensional (2D) heteronuclear Z-filtered correlation spectroscopy (Z-COSY) experiment

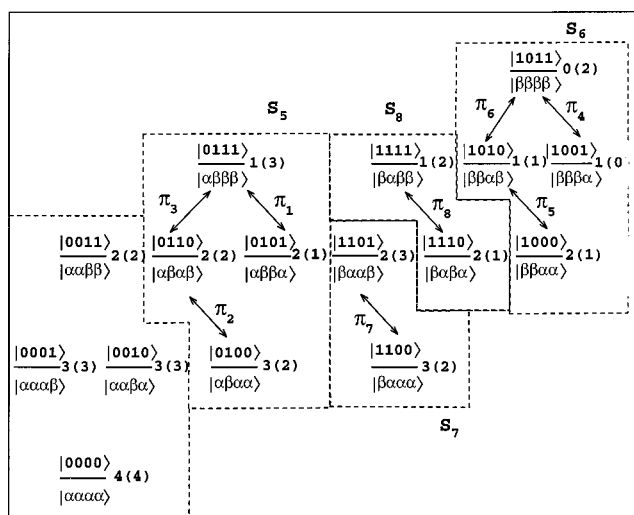


FIG. 5. Relabeled energy-level diagram for implementing a quantum full adder in the four-qubit system of 2–3 difluoro 6-nitrophenol. The maximal sets were created using the scheme outlines in Sec. II. The chains of elements in the maximal sets were mapped on to chains of states in this four-qubit system. To simplify the experimental protocol, it was noted that all the pulses that commute (which also means that they are not connected to a common energy level) can be applied simultaneously. The maximal sets are mutually exclusive and so the pulses of different sets commute with each other. This means that π_7 and π_8 of sets S_7 and S_8 can be applied simultaneously with the pulses of S_5 and S_6 . In the set S_5 , the labels of states $|\alpha\beta\beta\alpha\rangle$ and $|\alpha\beta\beta\beta\rangle$ were interchanged so that the pulses π_1 and π_2 can be applied simultaneously. Similarly, in S_6 , by interchanging the states $|\beta\beta\beta\alpha\rangle$ and $|\beta\beta\beta\beta\rangle$, π_4 and π_5 can be applied simultaneously. Hence, by this labeling, $\pi_1\pi_2\pi_4\pi_5\pi_7\pi_8$ followed by $\pi_3\pi_6$ would implement the quantum full adder. The initial (equilibrium) populations and final (after implementation of the full adder) populations are given beside each energy level as initial population (final population). The intensity of various transitions changes after the full adder. For example, we note that the intensity of the $\alpha\beta\beta$ transition of I_4 changes from +1 to –2, after implementation of the full adder.

was performed [30]. The sign of the peaks in the 2D spectrum yielded the connectivity matrix, which confirmed the assignments obtained by method (i).

To implement the quantum full adder using transition-selective pulses, we start with the system in equilibrium. While applying the selective pulses, we took some factors into consideration. First, the transition-selective pulses have to be tuned at a specific frequency with a narrow bandwidth so as to prevent the other lines from being perturbed. However, narrow bandwidth implies long pulses, which increase the experimental time and lead to relaxation-related errors. One has to optimize the experiment time so as to avoid errors due to relaxation. The schemes in Fig. 2(b) or Fig. 2 show that two of the four qubits have to be pulsed to implement full adder. The specific transitions to be pulsed are, however, far apart from each other with intermediate transitions between them. Hence, such a labeling would require pulsing individual transitions. Long duration pulses with high selectivity have to be used, the experiment would be lengthy, and relaxation will cause significant errors in the computation.

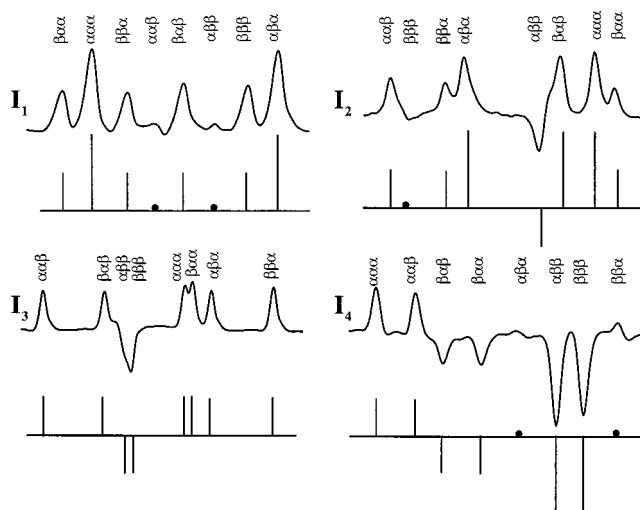


FIG. 6. Implementation of the quantum full adder in the four-qubit system of 2–3 difluoro 6-nitrophenol. Starting from equilibrium, three selective Gaussian-shaped pulses of lengths 50 μ s, 350 ms, and 450 ms were applied on selected transitions (as explained in text). Gradients were applied after each pulse to destroy any unwanted coherence created by the imperfection of pulses. A nonselective small flip-angle (5°) pulse was used to map the final populations. The experimental spectra are shown above with the expected spectra shown (as a stick diagram) below each spin. The intensities in the stick diagram are 0, ± 1 , and ± 2 corresponding to the final populations of Fig. 5. All the spectra are Fourier-transformed after multiplication of the signal with a Gaussian window function. The longitudinal relaxation rates for the four spins are $T_1^1=7$ s, $T_1^2=3.5$ s, $T_1^3=10$ s, and $T_1^4=4$ s. The observed experimental intensities are within 18% of the expected intensities.

On the other hand, by relabeling the energy levels suitably, the experimental protocol can be simplified. Figure 5 shows a relabeling which allows pulsing six transitions of one spin (I_4 of our system) followed by two transitions of the other spin (I_3 of our system). Moreover, these transitions were chosen such that they are adjacent to each other in the frequency spectrum and can be pulsed simultaneously, as given below.

First, we applied a spin-selective π pulse which inverted all the eight transitions of I_4 . Second, we applied another selective π pulse on two transitions (first two from the left in Fig. 4) of I_4 . The frequency of this selective pulse was tuned at the center of the two transitions and pulse power was adjusted to cause a π rotation of the two transitions. Thus, these two transitions get an effective rotation of 2π , whereas the other six transitions are rotated by π . The states connected by these two transitions have their equilibrium populations restored, while the states connected by the other six transitions will have their populations interchanged. Experimentally this scheme is preferred because it allows short duration pulses and faster implementation.

Subsequently, two pulses $\pi_3\pi_6$ were applied on two transitions of spin I_3 (fifth and sixth from the left in Fig. 4) as directed by our labeling scheme. After each selective pulse, a gradient was applied to kill any coherence created due to imperfection of radio frequency (rf) pulses. If one starts with the equilibrium state, the result is encoded in the final populations of different states. A nonselective small flip-angle (5°)

pulse was used to monitor the final populations. This pulse maps the population differences into the intensities of various transitions within a linear approximation. The obtained spectra are shown in Fig. 6, with expected results shown as a stick diagram underneath for each spin. The results have been reproduced within 18% of their expected intensities. The deviations from the expected intensities are due to relaxation and inhomogeneity of rf pulses. These spectra confirm the implementation of the quantum full adder operation.

VI. CONCLUSION

In this paper, we have outlined a protocol to find optimum labeling schemes for specific computations. While in quadrupolar systems OLS provides experimental schemes requiring fewer pulses, in spin- $\frac{1}{2}$ systems it helps to keep a better control over coherence and reduce experimental errors. This re-labeling has been utilized for implementation of the quantum full adder in a four-qubit spin- $\frac{1}{2}$ system by transition-selective pulses. The quantum full adder has also been realized using Hamiltonian evolution by Chuang *et al.* as a sub-routine of Shor's algorithm [17].

The search for higher qubits has inspired researchers to use homonuclear spin systems oriented in liquid crystalline matrices [22,31]. In such systems, the homonuclear spins can become strongly coupled and no longer be treated as qubits

[32]. Since the spins lose their identity as qubits, a conventional labeling scheme is not defined and the Hamiltonian evolution method is not applicable. It has been demonstrated that the 2^N eigenstates of N spin- $\frac{1}{2}$ strongly coupled nuclei can still be treated as an N -qubit system and quantum information processing can be performed using single-quantum transition-selective pulses [31]. In such systems, while the number of allowed single quantum transitions is more than that in weakly coupled systems, the number of transitions having significant (observable) intensities, in some cases, may be lower [33]. In such cases, OLS can be used to optimally label the eigenstates and perform computations utilizing observable single quantum transitions [30].

ACKNOWLEDGMENTS

The authors thank T. S. Mahesh, Rangeet Bhattacharya, N. Suryaprakash, and K. V. Ramanathan for useful discussions. The use of the DRX-500 NMR spectrometer funded by the Department of Science and Technology (DST), New Delhi, at the Sophisticated Instruments Facility, Indian Institute of Science, Bangalore, is also gratefully acknowledged. S. C. acknowledges the support of the IIT Roorkee. K.R. is grateful to the Indian Academy of Science, Bangalore for support. A.K. acknowledges "DAE-BRNS" for support and DST for a research grant for "Quantum Computing by NMR."

-
- [1] *The Physics of Quantum Information*, edited by D. Bouwnmeester, A. Ekert, and A. Zeilinger (Springer, Berlin, 2000).
- [2] M. A. Nielsen and I. L. Chuang, *Quantum Computation and Quantum Information* (Cambridge University Press, Cambridge, UK, 2000).
- [3] P. W. Shor, *SIAM Rev.* **41**, 303 (1999).
- [4] D. Deutsch and R. Jozsa, *Proc. R. Soc. London, Ser. A* **493**, 553 (1992).
- [5] L. K. Grover, *Phys. Rev. Lett.* **79**, 325 (1997).
- [6] E. M. Fortunato, M. A. Pravia, N. Boulant, G. Teklemariam, T. F. Havel, and D. G. Cory, *J. Chem. Phys.* **116**, 7599 (2002).
- [7] N. Boulant, K. Edmonds, J. Yang, M. A. Pravia, and D. G. Cory, *Phys. Rev. A* **68**, 032305 (2003).
- [8] Holly K. Cummins, Gavin Llewellyn, and Jonathan A. Jones, *Phys. Rev. A* **67**, 042308 (2003); H. K. Cummins and J. A. Jones, *New J. Phys.* **2**, 1 (2000).
- [9] N. A. Gershenfeld, and I. L. Chuang, *Science* **275**, 350 (1997).
- [10] D. G. Cory, M. D. Price, and T. F. Havel, *Physica D* **120**, 82 (1997).
- [11] Z. L. Madi, R. Bruschiweiler, and R. R. Ernst, *J. Chem. Phys.* **109**, 10 603 (1998).
- [12] I. L. Chuang, L. M. K. Vanderspyen, X. Zhou, D. W. Leung, and S. Llyod, *Nature (London)* **393**, 1443 (1998).
- [13] J. A. Jones and M. Mosca, *J. Chem. Phys.* **109**, 1648 (1998).
- [14] Kavita Dorai, Arvind and Anil Kumar, *Phys. Rev. A* **61**, 042306 (2000).
- [15] T. S. Mahesh, Kavita Dorai, Arvind and Anil Kumar, *J. Magn. Reson.* **148**, 95 (2001).
- [16] I. L. Chuang, N. Gershenfeld, and M. Kubinec, *Phys. Rev. Lett.* **80**, 3408 (1998).
- [17] L. M. K. Vanderspyen, Matthias Steffen, Gregory Breyta, C. S. Yannoni, M. H. Sherwood, and I. L. Chuang, *Nature (London)* **414**, 883 (2001).
- [18] Ranabir Das, T. S. Mahesh, and Anil Kumar, *Phys. Rev. A* **67**, 062304 (2003).
- [19] Ranabir Das, Avik Mitra, Vijay Kumar S, and Anil Kumar, *Int. J. Quantum Inf.* **1**, 387 (2003).
- [20] Neeraj Sinha, T. S. Mahesh, K. V. Ramanathan, and Anil Kumar, *J. Chem. Phys.* **114**, 4415 (2002).
- [21] K. V. R. M. Murali, Neeraj Sinha, T. S. Mahesh, Malcom Levitt, K. V. Ramanathan, and Anil Kumar, *Phys. Rev. A* **66**, 022313 (2002).
- [22] Anil Kumar, K. V. Ramanathan, T. S. Mahesh, Neeraj Sinha, and K. V. R. M. Murali, *Pramana* **59**, 243 (2002).
- [23] Ranabir Das, T. S. Mahesh, and Anil Kumar, *J. Magn. Reson.* **159**, 46 (2002).
- [24] T. S. Mahesh, Ph.D. thesis, Indian Institute of Science, Bangalore (2003).
- [25] A. K. Khitrin and B. M. Fung, *J. Chem. Phys.* **112**, 6963 (2000).
- [26] A. Khitrin, H. Sun, and B. M. Fung, *Phys. Rev. A* **63**, 020301(R) (2001).
- [27] A. K. Khitrin and B. M. Fung, *Phys. Rev. A* **64**, 032306 (2001).
- [28] Ranabir Das and Anil Kumar, *Phys. Rev. A* **68**, 032304 (2003).
- [29] Reference [32], p. 221.
- [30] Ranabir Das, Rangeet Bhattacharya, and Anil Kumar, *J. Magn. Reson.* (to be published).

- [31] T. S. Mahesh, Neeraj Sinha, Arindam Ghosh, Ranabir Das, N. Suryaprakash, Malcolm H. Levitt, K. V. Ramanathan, and Anil Kumar, *Curr. Sci.* **85**, 932 (2003).
- [32] R. R. Ernst, G. Bodenhausen, and A. Wokaun, *Principles of*

Nuclear Magnetic Resonance in One and Two Dimensions (Clarendon, Oxford, UK, 1987).

- [33] P. Diehl and C. L. Khetrapal, *NMR-Basic Principles and Progress* (Springer-Verlag, New York, 1969), Vol. 1.